Available online at www.sciencedirect.com
ScienceDirect
Polymer 48 (2007) 82–90
polymer
www.elsevier.com/locate/polymer

Stimuli-responsive polymers. 9. Photo-regulation of optical rotations in chiral polyesters: Altering responsive outputs with conformationally flexible backbone elements

Gary D. Jaycox*

DuPont Central Research and Development, Biochemical Science and Engineering, E328-205B Experimental Station, Wilmington, DE 19880-0328, USA

Received 21 August 2006; received in revised form 2 November 2006; accepted 3 November 2006
Available online 1 December 2006

Abstract

Conformationally restricted polyesters comprising alternating azobenzene and chiral binaphthylene main-chain units undergo photo-induced oscillations in optical rotatory power when stimulated with sequential intervals of ultraviolet and visible light exposure. The incorporation of flexible (oligo)ethylene oxide backbone segments into these constructs has resulted in a new family of materials having vastly altered photo-responsive chiroptical properties. Light-regulated outputs were found to be strongly dependent upon the length of the flexible backbone segments employed and on their specific locations of placement within the polyester chain. Most notably, the insertion of flexible oligo(ethylene oxide) spacer elements between neighboring binaphthylene and azobenzene main-chain units had a pronounced damping effect on the photo-dynamic behavior exhibited by these chiral systems. Similar results were noted for a related series of oligomeric model compounds that were specifically designed to mimic local monomer sequences present within the larger polyester structures.

Keywords: Azo polymers; Optical rotation; Light-regulated chiroptical response

1. Introduction

Polymers and oligomers that contain atropisomeric *R*- or *S*-2,2′-binaphthylene segments exhibit novel chiroptical properties that stem from their conformationally dynamic, three-dimensional architectures [1]. The inclusion of main-chain azobenzene stimuliphores into macromolecules of this kind allows for the controlled disruption of local and more global backbone geometries via a series of light-modulated *trans*–*cis*-isomerization events. As reported earlier [2–11], these reversible structural changes often lead to dramatic fluctuations in optical rotatory power and circular dichroism spectra that are strongly correlated to the nature of the solvent medium and other environmental influences. Properly designed, these photo-responsive materials are potentially well suited for the fabrication of sensors and optical switching and recording elements that have relevance to a number of emerging technologies.

Previous studies carried out in this laboratory have demonstrated that photo-regulated chiroptical changes tend to be most pronounced for macromolecular constructs that are endowed with conformationally restricted main-chain geometries [2–8]. In these systems, steric and electronic perturbations afforded by local *trans*–*cis*-azobenzene isomerization reactions are efficiently transmitted throughout the larger polymer structure. As shown in Fig. 1, levorotatory specific rotations recorded for polyester **1R** dissolved in THF oscillate over a span of several hundred deg dm^{-1} g^{-1} cm^3 when this system is stimulated by multiple UV light–visible light illumination cycles. This chiroptical output can be conveniently monitored at the sodium D-line (589 nm) and is thus well removed from the dual ‘‘input’’ light frequencies that serve to drive the polymer’s response. Similar results have been

* Tel.: +1 302 695 7138; fax: +1 302 695 9799.
E-mail address: gary.d.jaycox@usa.dupont.com

0032-3861/$ - see front matter © 2006 Elsevier Ltd. All rights reserved.
doi:10.1016/j.polymer.2006.11.006

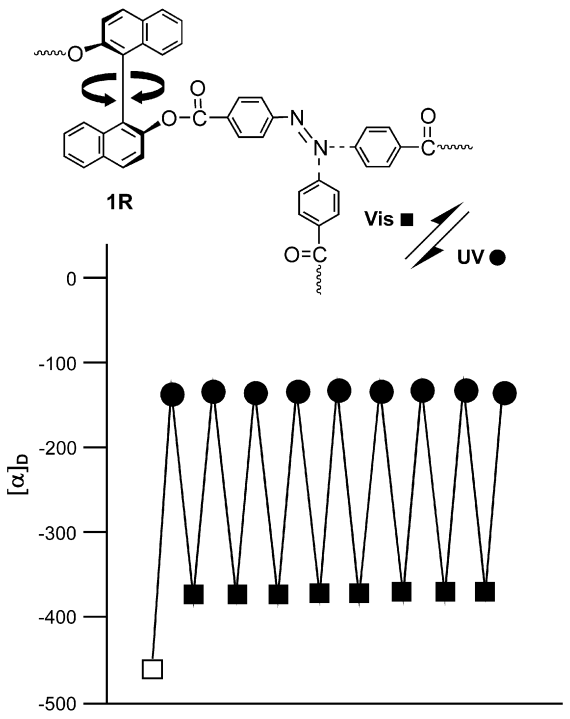

Fig. 1. Photo-regulated chiroptical response for the conformationally restricted polyester **1R** evaluated in THF. Graph shows D-line specific rotations for the dark-adapted state (□) and those recorded after multiple UV (●) and visible (■) light exposure steps.

obtained for a number of related polyaramide [3–7], polyether [8] and polyurethane [12] analogues that also contain tightly coupled azobenzene and chiral binaphthylene main-chain units.

Macromolecular variants endowed with more flexible backbone architectures are likely to have significantly altered light-responsive outputs. Here, isomerization-induced perturbations supplied by the azobenzene stimuliphores may be partially screened or dampened-out along the polymer chain. In an effort to test these predictions and to uncover additional structure–property relationships that characterize this class of photo-dynamic materials, we have now synthesized a new series of polymeric and oligomeric analogues [13,14] that are fitted with flexible (oligo)ethylene oxide backbone segments. As will be discussed below, the photo-regulated changes in optical rotatory power that are observed for these new materials are strongly dependent upon the length of the flexible backbone elements employed and upon their specific locations of placement within the polyester chain.

2. Experimental

2.1. Materials

Polyester *trans*-**1R** and the monomer *trans*-azobenzene-4,4′-dicarbonyl chloride were prepared as described earlier [8,15]. (*R*)-(+)-1,1′-Bi-2-naphthol (99%, Aldrich) was recrystallized from warm methanol and then rigorously dried in vacuo before use. Anhydrous tetrahydrofuran (THF), *N*,*N*-dimethylformamide (DMF) and *N*,*N*-dimethylacetamide (DMAC) (Aldrich) were stored under Ar over 4 Å molecular sieves. All other reagents and solvents (>97%) were obtained from Aldrich and were used without further purification.

2.2. Monomer syntheses

2.2.1. Binaphthylene monomer *2R*

A stirred solution of *R*-(+)-1,1′-bi-2-naphthol (10.0 g, 34.9 mmol), 2-chloroethanol (14.0 g, 174 mmol) and potassium carbonate (24.1, 174 mmol) in anhydrous DMF (80 mL) was heated to reflux under Ar for 24 h. The reaction mixture was poured into a brine solution (300 mL) giving a sticky tan precipitate. The solid was dissolved into chloroform (250 mL) and extracted with water (3 × 100 mL) and brine (100 mL) and then concentrated in vacuo to give a viscous tan oil. The oil was dissolved into a hot methanol–water solution (70:30 v:v, 200 mL). On cooling, the solution deposited **2R** (81%) as an off-white crystalline solid. Mp. 131–133 °C (lit. [16] Mp. 131–134 °C); Proton NMR: (DMSO-d_6, 500 MHz) δ 8.04 (d, 2H), 7.92 (d, 2H), 7.61 (d, 2H), 7.30–7.35 (m, 2H), 7.18–7.22 (m, 2H), 6.92 (d, 2H), 4.52 (t, 2H), 4.02 (t, 4H), 3.39–3.44 (m, 4H); MS: *m/e* 375 ([M]H$^+$); $[\alpha]_D^{25} = (-)24.1$ ($c = 0.870$ g/dL, THF).

2.2.2. Binaphthylene monomer *3R*

This monomer was prepared from 2-(2-chloroethoxy)ethanol and *R*-(+)-1,1′-bi-2-naphthol in a manner similar to that described for the synthesis of **2R** above. Monomer **3R** was purified by column chromatography (silica) using THF as a mobile phase. The product was isolated (71%) as a viscous tan oil. Proton NMR: (DMSO-d_6, 500 MHz) δ 8.03 (d, 2H), 7.92 (d, 2H), 7.60 (d, 2H), 7.30–7.35 (m, 2H), 7.18–7.23 (m, 2H), 6.97 (d, 2H), 4.40 (t, 2H), 4.10–4.16 (m, 4H), 3.40–3.46 (m, 4H), 3.23–3.30 (m, 4H), 3.08–3.15 (m, 4H); FTIR (neat): 3426 cm^{-1} (OH stretch, br); MS: *m/e* 463 ([M]H$^+$); $[\alpha]_D^{25} = (+)27.1$ ($c = 0.558$ g/dL, THF).

2.2.3. Binaphthylene monomer *4R*

This monomer was prepared from 2-[2-(2-chloroethoxy)-ethoxy]ethanol and *R*-(+)-1,1′-bi-2-naphthol in a manner similar to that described for the synthesis of **2R** above. Monomer **4R** was purified by column chromatography (silica) using THF–ethyl ether (50:50 v:v) as a mobile phase. The product was isolated (65%) as a viscous tan oil. Proton NMR: (DMSO-d_6, 500 MHz) δ 8.03 (d, 2H), 7.92 (d, 2H), 7.60 (d, 2H), 7.30–7.35 (m, 2H), 7.18–7.23 (m, 2H), 6.97 (d, 2H), 4.51 (t, 2H), 4.11 (t, 4H), 3.39–3.49 (m, 8H) 3.28–3.32 (m, 4H), 3.11–3.21 (m, 8H); FTIR (neat): 3421 cm^{-1} (OH stretch, br); MS: *m/e* 551 ([M]H$^+$); $[\alpha]_D^{25} = (+)26.8$ ($c = 0.041$ g/dL, THF).

2.3. Polymer syntheses

2.3.1. Polyester trans-*5R*

A stirred solution of **2R** (1.25 g, 3.34 mmol) and *trans*-azobenzene-4,4′-dicarbonyl chloride (1.08 g, 3.51 mmol) in

anhydrous DMAC (75 mL) was treated with several drops of pyridine and then heated to reflux for 24 h in the dark under Ar. The reaction mixture was concentrated in vacuo to a volume near 25 mL and then poured into water (100 mL) giving an orange precipitate. The solid was collected by filtration and dissolved into chloroform (200 mL). The chloroform solution was extracted with water (3 × 100 mL) and brine (50 mL), dried over anhydrous sodium sulfate and then concentrated in vacuo giving an orange foam. The product was re-dissolved into THF (20 mL), precipitated from hexanes (100 mL) and finally dried in vacuo at 50 °C for 24 h to give *trans*-**5R** as a coarse orange solid: FTIR (film): 1715 cm^{-1} (C═O ester stretch); $[\alpha]_D^{25} = (+)30.7$ ($c = 0.0651$ g/dL, THF).

2.3.2. Polyester trans-*6R*

This polymer was prepared from monomers **4R** and *trans*-azobenzene-4,4′-dicarbonyl chloride in a manner similar to that described for the synthesis of polyester *trans*-**5R** above. FTIR (film): 1716 cm^{-1} (C═O ester stretch); $[\alpha]_D^{25} = (+)23.0$ ($c = 0.0440$ g/dL, THF).

2.3.3. Polyester trans-*7R*

A stirred solution of *R*-(+)-1,1′-bi-2-naphthol (0.50 g, 1.75 mmol) in anhydrous THF (50 mL) at 0 °C was treated with two molar equivalents of *n*-butyl lithium (2.5 M in hexanes). Monomer *trans*-azobenzene-4,4′-dicarbonyl chloride (1.08 g, 3.52 mmol) dissolved into anhydrous THF (20 mL) was next added over a 20-min period. The reaction mixture was warmed to room temperature, treated with diethylene glycol (0.185 g, 1.74 mmol) and several drops of pyridine and then heated to reflux for 24 h in the dark under Ar. The reaction mixture was concentrated in vacuo to a volume near 25 mL and then poured into water (100 mL) giving an orange precipitate. The solid was collected by filtration and dissolved into chloroform (200 mL). The chloroform solution was extracted with water (3 × 100 mL) and brine (100 mL), dried over anhydrous sodium sulfate and then concentrated in vacuo giving an orange foam. The product was re-dissolved into THF (20 mL), precipitated from hexanes (100 mL) and finally dried in vacuo at 50 °C for 24 h to give *trans*-**7R** as a coarse orange solid. FTIR (film): 1732 cm^{-1} (C═O ester stretch, br); $[\alpha]_D^{25} = (-)331$ ($c = 0.0390$ g/dL, THF).

2.3.4. Polyester trans-*8R*

This random copolymer was prepared from the monomers *R*-(+)-1,1′-bi-2-naphthol, *trans*-azobenzene-4,4′-dicarbonyl chloride and hexaethylene glycol in a manner similar to the synthesis of polyester *trans*-**7R** described above. FTIR (film): 1738 cm^{-1} (C═O ester stretch, br); $[\alpha]_D^{25} = (-)219$ ($c = 0.0762$ g/dL, THF).

2.4. Model compound syntheses

2.4.1. Model compound trans-*9R*

A stirred solution of *R*-(+)-1,1′-bi-2-naphthol (1.00 g, 3.49 mmol) and *trans*-4-(phenylazo)benzoyl chloride (1.88 g, 7.68 mmol) in anhydrous DMAC (40 mL) was treated with several drops of pyridine and then heated to reflux for 24 h in the dark under Ar. The reaction mixture was concentrated in vacuo giving a crude red-orange solid. The solid was dissolved into chloroform (300 mL) and extracted sequentially with 10% aqueous sodium carbonate (2 × 50 mL), water (4 × 100 mL) and brine (50 mL), dried over anhydrous sodium sulfate and then concentrated in vacuo giving an orange foam. The product was purified in the dark by column chromatography (silica) using a mixture of ethyl ether–hexanes (40:60 v:v) as the mobile phase. After drying in vacuo at 50 °C for 48 h, *trans*-**9R** was isolated (86%) as a bright orange solid. Proton NMR: (DMSO-d_6, 500 MHz) δ 8.17–8.20 (m, 2H), 8.07–8.10 (m, 2H), 7.88–7.92 (m, 4H), 7.71–7.82 (m, 10H), 7.59–7.62 (m, 6H), 7.52–7.59 (m, 2H), 7.41–7.45 (m, 2H), 7.26–7.30 (m, 2H); FTIR (film): 1738 cm^{-1} (C═O stretch); MS: *m/e* 703 ($[M]H^+$); $[\alpha]_D^{25} = (-)193$ ($c = 0.0424$ g/dL, THF).

2.4.2. Model compound trans-*10R*

A stirred solution of **2R** (1.20 g, 3.20 mmol) and *trans*-4-(phenylazo)benzoyl chloride (1.65 g, 6.74 mmol) in anhydrous DMAC (40 mL) was treated with several drops of pyridine and then heated to reflux for 24 h in the dark under Ar. The reaction mixture was concentrated in vacuo giving a crude orange solid. The product was dissolved into chloroform (100 mL), extracted with water (3 × 100 mL) and brine (50 mL), dried over anhydrous sodium sulfate and then concentrated in vacuo giving an orange foam. The product was purified in the dark by column chromatography (silica) using ethyl ether as a mobile phase. After drying in vacuo at 55 °C for 24 h, *trans*-**10R** was isolated (80%) as a bright red-orange solid. Proton NMR: (DMSO-d_6, 500 MHz) δ 8.05 (d, 2H), 7.90–7.93 (m, 6H), 7.80–7.83 (m, 4H), 7.69–7.73 (m, 4H), 7.61–7.64 (m, 8H), 7.25–7.30 (m, 2H), 7.15–7.19 (m, 2H), 6.93–6.95 (m, 2H), 4.30–4.38 (t, 4H), 4.26–4.48 (t, 4H); FTIR (film): 1716 cm^{-1} (C═O stretch); MS: *m/e* 791 ($[M]H^+$); $[\alpha]_D^{25} = (+)39.4$ ($c = 0.0279$ g/dL, THF).

2.4.3. Model compound trans-*11R*

This derivative, isolated as a bright red-orange solid, was prepared from *trans*-4-(phenylazo)benzoyl chloride and monomer **3R** in a manner similar to the synthesis of *trans*-**10R** described above. Proton NMR: (DMSO-d_6, 500 MHz) δ 8.03–8.08 (m, 4H), 7.98–8.00 (m, 2H), 7.89–7.95 (m, 10H), 7.58–7.64 (m, 8H), 7.28–7.31 (m, 2H), 7.19–7.22 (m, 2H), 6.95–7.00 (m, 2H), 4.15–4.19 (t, 4H), 4.09–4.12 (t, 4H), 3.49–3.53 (m, 4H), 3.30–3.38 (m, 4H); FTIR (film): 1715 cm^{-1} (C═O stretch); MS: *m/e* 879 ($[M]H^+$); $[\alpha]_D^{25} = (+)38.8$ ($c = 0.0696$ g/dL, THF).

2.4.4. Model compound trans-*12R*

This derivative, isolated as a red-orange, viscous oil, was prepared from *trans*-4-(phenylazo)benzoyl chloride and monomer **4R** in a manner similar to the synthesis of *trans*-**10R** described above. Proton NMR: (DMSO-d_6, 500 MHz) δ 8.10–8.12 (m, 4H), 7.87–7.99 (m, 12H), 7.60–7.64 (m, 6H), 7.51–7.53 (m, 2H), 7.28–7.31 (m, 2H), 7.20–7.23 (m,

2H), 6.91–7.95 (m, 2H), 4.31–4.35 (t, 4H), 4.06–4.08 (t, 4H), 3.59–3.62 (m, 4H), 3.39–3.41 (t, 4H), 3.27–3.29 (t, 4H), 3.13–3.18 (m, 4H); FTIR (neat): 1720 cm^{-1} (C=O stretch); MS: *m/e* 967 ($[M]H^+$); $[\alpha]_D^{25} = (+)19.9$ ($c = 0.156$ g/dL, THF).

2.5. Analytical methods

Melting points were determined in open capillary tubes with a Laboratory Devices (Holliston, MA) Mel-Temp unit and are uncorrected. A heating rate of 2 °C/min was consistently employed. Proton nuclear magnetic resonance (^1H NMR) spectra were acquired at 500 MHz on a Bruker Advance DRX-500 instrument. Tetramethylsilane was employed as a standard. Fourier transform infrared (FTIR) spectra were recorded on a Perkin Elmer 1600 series spectrophotometer. Samples were typically measured in thin-film form. High resolution electron impact mass spectra were furnished with a VG 70-250SE double-focusing mass spectrometer. UV–visible (UV–Vis) spectra were obtained with a Hewlett Packard 8453 UV–Vis spectrophotometer. Gel permeation chromatography (GPC) employed for polymer molecular weight determination was carried out with a Waters HPLC 150C equipped with a refractive index detector. Polymer samples were dissolved into DMAC containing trace amounts of Ionol (antioxidant) and toluene sulfonic acid. Measurements were run at 135 °C and narrow molecular weight polystyrene standards were utilized for the purposes of GPC calibration. Glass transition temperatures were determined by temperature-modulated differential scanning calorimetry (DSC) using a TA Instruments 2920 DSC. Polymer samples were heated at a base rate of 5 °C/min with a temperature modulation of +/−0.5 °C applied every 40 s. All thermal measurements were performed under nitrogen.

Specific rotations, reported here as deg dm^{-1} g^{-1} cm^3, were evaluated at the sodium D-line (589 nm) with a Perkin Elmer Model 241 polarimeter. Polymer samples were dissolved in specified solvents at concentrations near 0.050 g/dL unless otherwise indicated. Standard 10 cm pathlength cells were utilized for all measurements. Polarimetry cells were connected to a thermostated circulating bath (VWR model 1166) maintained at a constant temperature of 25 °C.

Low intensity UV irradiations of polymer solutions were performed with a Blak-Ray Long Wavelength UV lamp (San Gabriel, CA; Model B 100 AP). The maximum intensity of light output was centered near 360 nm. Visible light illuminations were carried out with a Scientific Instruments Dyna-Lume Sun-Lite I Illuminator (Skokie, IL; Model 240-190). Solutions were illuminated for 15-min intervals with near-UV light or visible light while confined within stoppered polarimetry cells. Lamp-to-sample path lengths were typically 6–8 cm. Polymer solutions were maintained near room temperature during all irradiation procedures. When required, a combination of optical cut-on and band-pass filters (Oriel Corp., Stratford, CT) was utilized to furnish radiation within a desired spectral window.

3. Results and discussion

3.1. R-Binaphthylene diol syntheses

The chiral binaphthylene monomers **2R**–**4R** fitted with extended (oligo)ethylene oxide arm segments were synthesized efficiently from commercially available *R*-(+)-1,1′-bi-2-naphthol as depicted in Scheme 1. The reaction conditions utilized for the preparation of **2R**–**4R** were specifically chosen to minimize the unwanted racemization of the *R*-binaphthylene ring system. Earlier work by Cram [17] demonstrated that, under sufficiently basic conditions, the two phenolic groups in chiral 1,1′-bi-2-naphthols can simultaneously exist in their deprotonated states. The presence of twin negative charges within the binaphthylene molecule appears to favor an elongation of its 1,1′-biaryl bond that can lead to a diminished rotational energy barrier for racemization. The potential for racemization during base-mediated transformations of *R*-(+)-1,1′-bi-2-naphthol was investigated by Stock and Kellogg [16]. As part of their study, a number of different reaction conditions for the preparation of **2R** and other chiral bis-alkylated products were directly explored. When K_2CO_3 was employed as base in a hot DMF solvent medium, the authors found that racemization of the axially dissymmetric binaphthylene ring was greatly suppressed, falling below 2% as evidenced by a series of HPLC measurements. Under these conditions, the mono-alkylation reaction proceeded rapidly relative to the rate of racemization for the *R*-bi-2-naphthol starting material. In our laboratory, **2R** prepared by the K_2CO_3/DMF route outlined in Scheme 1 possessed a specific rotation value and a crystalline melting point that were identical to those reported earlier [16] for this chiral derivative. Moreover, the use of lower temperatures and/or shorter reaction times to promote these transformations furnished bis-alkylated products having experimentally equivalent optical rotation values, although the desired monomers were isolated in lower preparative yields. Our observations, when coupled with those reported earlier by Stock and Kellogg [16], provide good evidence that chiral monomers **2R**–**4R** prepared in this study were characterized by high degrees of optical purity.

Following the K_2CO_3 mediated bis-alkylation reactions, the diol monomers **3R** and **4R** were isolated as viscous oils after purification by column chromatography. Product **2R** fitted with shorter arm units was obtained as a low-melting crystalline solid after recrystallization from aqueous methanol. The

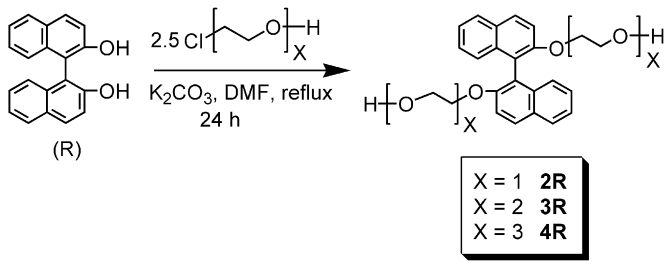

Scheme 1. Synthesis of extended *R*-binaphthylene diol monomers.

chiral diols **3R** and **4R** were characterized by small dextrorotatory specific rotations falling near (+)27° $dm^{-1}\,g^{-1}\,cm^3$ when evaluated at the sodium D-line in THF. Interestingly, these values are similar to the rotation of (+)36° $dm^{-1}\,g^{-1}\,cm^3$ recorded for the *R*-(+)-1,1′-bi-2-naphthol starting material. In stark contrast, diol **2R** was found to be weakly levorotatory, affording a specific rotation of (−)24° $dm^{-1}\,g^{-1}\,cm^3$ when examined under the same set of experimental conditions.

3.2. Polymer synthesis and characterization

Four chiral polyester analogues containing flexible (oligo)-ethylene oxide main-chain segments were prepared as part of this study. Twin polycondensation reactions involving *trans*-azobenzene-4,4′-dicarbonyl chloride and the extended *R*-binaphthylene diols **2R** and **4R** were utilized to furnish copolyesters *trans*-**5R** and *trans*-**6R**, respectively (Scheme 2). The polymerizations were carried out in anhydrous DMAC at elevated temperatures in the presence of catalytic quantities of pyridine. When compared to the conformationally restricted polyester **1R** depicted in Fig. 1, polyester variant *trans*-**5R** possessed a periodic repeat structure with short ethylene oxide spacer segments directly interposed between neighboring binaphthylene and *trans*-azobenzene backbone segments. A similar periodic sequence of monomer units was engineered into copolyester *trans*-**6R**. In this case, the length of the spacer element was increased three-fold to further enhance the conformational flexibility of this polyester's backbone.

Polyester constructs *trans*-**7R** and *trans*-**8R** containing randomly positioned oligo ethylene oxide backbone segments were prepared from *R*-(+)-1,1′-bi-2-naphthol as shown in Scheme 3. Here, two molar equivalents of *n*-butyl lithium were utilized to generate nucleophilic phenoxide-like species that efficiently coupled with the *trans*-azobenzene-4,4′-dicarbonyl chloride monomer. This approach initially furnished a series of lower molecular weight oligomers that were subsequently chain-extended with diethylene glycol or hexaethylene glycol to give the desired copolyester analogues. As for the conformationally restricted polyester *trans*-**1R** depicted in

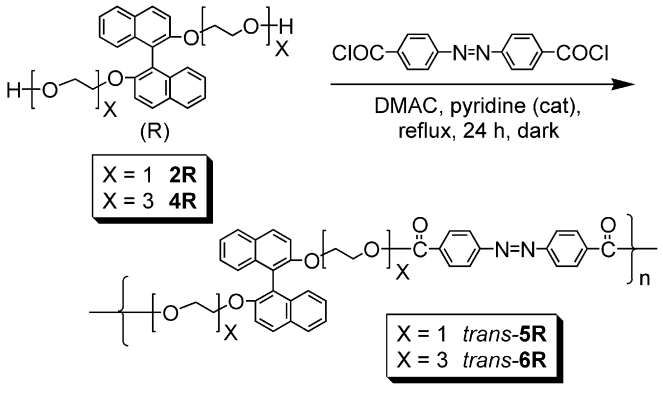

Scheme 2. Synthesis of periodic copolyester constructs *trans*-**5R** and *trans*-**6R**.

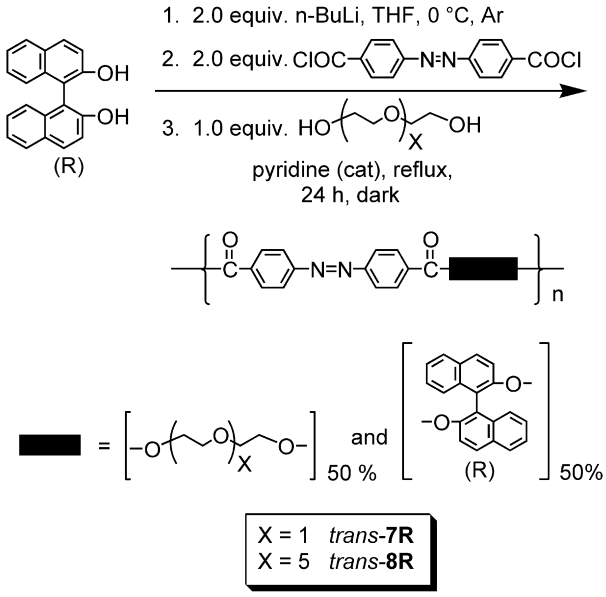

Scheme 3. Synthesis of random copolyester constructs *trans*-**7R** and *trans*-**8R**.

Fig. 1, the monomer sequences present in random copolymers *trans*-**7R** and *trans*-**8R** allowed for the direct coupling of adjacent binaphthylene and azobenzene units along each polymer chain.

The four polyester constructs were isolated as orange solids exhibiting coarse fibrous textures at room temperature. The *trans*-azobenzene loadings in these new materials varied from about 23 to 42 wt% as evidenced by ^{1}H NMR spectroscopy. Within this copolymer series, (oligo)ethylene oxide and chiral binaphthylene segment contents varied inversely, with *trans*-**6R** and *trans*-**8R** having the highest weight percentages of flexible backbone elements (Table 1). The periodic variant *trans*-**6R** exhibited a relatively low glass transition temperature (T_g) near 36 °C. In stark contrast, the other *trans*-copolymers endowed with either periodic or random monomer sequences were characterized by elevated T_g values that more closely approximated the T_g measured for the wholly aromatic polyester derivative *trans*-**1R** (Table 2). These results are consistent with the presence of conformationally "soft" triethylene oxide spacer segments in *trans*-**6R** that effectively serve to de-couple the polymer's more rigid binaphthylene and *trans*-azobenzene main-chain units, thus providing globally for a more flexible backbone structure (Scheme 2). That periodic copolymer *trans*-**5R** exhibited a T_g above 90 °C would

Table 1
Weight-percent loadings of azobenzene, *R*-binaphthylene and flexible (oligo)-ethylene oxide fragments in polyester backbones

Polyester	Azobenzene[a]	*R*-Binaphthylene[a]	(Oligo)ethylene oxide[a]
1R	34.6	48.5	0
5R	29.6	41.5	19.7
6R	23.0	32.2	37.8
7R	41.9	29.3	12.1
8R	34.8	24.3	27.0

[a] Theoretical values consistent with ^{1}H NMR data.

Table 2
Glass transition temperatures and molecular weight data for *trans*-polyesters

Polyester (*trans*-)	T_g[a] (°C)	M_n[b]	M_w/M_n[b]
1R	141	9400	2.1
5R	93	7700	2.4
6R	36	7300	2.3
7R	130	10,100	2.6
8R	99	9300	2.4

[a] Determined by temperature-modulated DSC under nitrogen.
[b] Determined by GPC in DMAC.

Table 3
D-line specific rotation values for *trans*-polyester analogues in different solvent media

Polymer (*trans*-)	$[\alpha]_D^{25}$ (deg dm^{-1} g^{-1} cm^3)		
	THF	DMAC	$CHCl_3$
1R	(−)462	(−)438	(−)409
5R	(+)31	(+)40	(−)2
6R	(+)23	(+)28	(+)17
7R	(−)331	(−)264	(−)260
8R	(−)219	(−)218	(−)210

seem to indicate that its shorter ethylene oxide spacers are less effective in this regard. Similar reductions in glass transition temperatures would not be expected for *trans*-**7R** and *trans*-**8R** where random backbone structures allow for the direct connectivity of adjacent binaphthylene and azobenzene groups along each polyester chain (Scheme 3). As prepared, all of the copolymers were characterized by relatively low molecular weight values. Number-averaged molecular weights assessed by GPC (in DMAC) ranged between 7300 and 10,100 with polydispersities falling near 2.4. These findings are consistent with earlier polycondensation reactions involving other 2,2′-disubstituted binaphthylene monomers that have also tended to furnish lower molecular weight products [6,9]. As for the parent polyester *trans*-**1R** described above, *trans*-copolymers **5R**–**8R** were readily dissolved by a number of organic solvents suitable for chiroptical measurements, including DMAC, THF, 1,4-dioxane and chloroform.

3.3. Specific rotations for the trans-azobenzene modified copolymers

For many axially dissymmetric binaphthylene derivatives, there exists a close correspondence between the rotational state of the atropisomeric molecule and the chiroptical properties that it ultimately displays in solution [18–21]. Cisoid and transoid orientations of the twin naphthylene rings are both possible, depending upon the nature of their ring substituents and the particular solvent into which each chiral binaphthylene derivative is placed. For this reason, macromolecules that are fashioned from multiple *R*- or *S*-binaphthylene segments tend to exhibit optical rotations and circular dichroism spectra that are strongly influenced by a range of structural and environmental factors [1].

The *trans*-azobenzene modified copolyesters described in this study were characterized by both levorotatory and dextrorotatory specific rotations even though they were all constructed from the same *R*-(+)-1,1′-bi-2-naphthol building-block. Specific rotation values gathered in three different solvent media are compiled in Table 3 for this polymer series. Rotational data for polyester *trans*-**1R** acquired as part of an earlier study [8] are also included for comparison. When evaluated in THF, the random copolymers *trans*-**7R** and *trans*-**8R** were characterized by strong levorotatory rotations that fell near (−)331 and (−)219° dm^{-1} g^{-1} cm^3. These values were somewhat reduced in their respective magnitudes when compared to the rotation of (−)462° dm^{-1} g^{-1} cm^3 measured earlier [8] for polyester *trans*-**1R**. This behavior is consistent with diminished *R*-binaphthylene backbone contents within *trans*-**7R** and *trans*-**8R** relative to that present in the parent polyester analogue (see Table 1). Interestingly, the specific rotations recorded for copolymer variants *trans*-**5R** and *trans*-**6R** were found to be vastly different. The two periodic constructs having flexible spacer elements directly attached to each binaphthylene main-chain unit displayed relatively weak dextrorotatory rotations of (+)31 and (+)23° dm^{-1} g^{-1} cm^3 when evaluated under the same set of experimental conditions. Similar trends in measured optical rotatory power were observed in DMAC and chloroform for most of this polymer series (Table 3). Polyester *trans*-**5R** provided a single exception, undergoing an inversion in its rotational behavior when it was examined in the chlorinated solvent medium.

3.4. Photo-regulation of optical rotations

The photo-dynamic properties of disubstituted azobenzenes continue to be widely exploited for the development of new materials with light-responsive molecular geometries. For many azobenzene modified derivatives, photostationary state *trans*–*cis*-isomer ratios can be reliably cycled between two extremes by sequentially irradiating the chromophore's π–π* band with near-UV light (*cis*-enriched) and its lower energy n–π* band with visible light (*trans*-enriched). Reversible inter-conversions between the linear *trans* and kinked *cis*-isomeric states triggered by this dual irradiation scheme proceed efficiently in solution and are devoid of competing photo-processes that can lead to unwanted fatiguing or hysteresis effects [22,23]. When covalently coupled into a polymer backbone that is comprising multiple atropisomeric binaphthylene segments, the azobenzene group can thus serve as photonically driven molecular actuator or stimuliphore, allowing for the dynamic control of chiral macromolecular architectures over both local and more global length scales [7,8]. For conformationally restricted polymers like **1R** depicted in Fig. 1, the photo-actuated chiroptical responses that are generated in this manner can be quite dramatic, with specific rotations shifting by several hundred deg dm^{-1} g^{-1} cm^3 or even inverting to the opposite sign under certain experimental conditions [8].

The incorporation of flexible (oligo)ethylene oxide main-chain segments into the polyester backbone to give constructs **5R**–**8R** had a measurable impact on photo-regulated

chiroptical behaviors. Light-responsive outputs were strongly influenced both by the length of the flexible backbone elements employed and by their specific locations of placement within the polyester chain. Chiroptical data for this new copolymer series dissolved in THF are summarized graphically in Fig. 2 and can be compared to that gathered earlier [8] for the more conformationally rigid polyester **1R** (Fig. 2 – far left). As can be noted, the strong levorotatory rotation initially recorded for random copolyester *trans*-**7R** was significantly diminished following the UV irradiation step that provided a new *trans–cis* photostationary state composition enriched in the higher energy *cis*-isomer. The illumination of **7R** with visible light served to trigger the reverse *cis*-to-*trans* isomerization process along the polymer's backbone, partially restoring its specific rotation to a value near (−)272° $dm^{-1}\,g^{-1}\,cm^3$. This photo-regulated oscillatory response in optical rotatory power spanned a range of about 120° $dm^{-1}\,g^{-1}\,cm^3$ and was about half that observed for polyester **1R** that possessed twice the loading of chiral *R*-binaphthylene linkages. Copolyester **8R** randomly fitted with longer hexaethylene oxide main-chain units behaved similarly, with its specific rotation fluctuating by more than 95° $dm^{-1}\,g^{-1}\,cm^3$ when stimulated by the same dual UV light–visible light illumination scheme (Fig. 2). Importantly, these results indicate that the random insertion of conformationally flexible elements into the polyester backbone does not lead to a different mode of stimuli-responsive behavior for this class of chiral materials as long as the covalent connectivity of adjacent binaphthylene and azobenzene groups is maintained.

The light-responsive profiles exhibited by the periodic copolyesters **5R** and **6R** were found to be radically very different as indicated in Fig. 2. Following the UV light exposure step, the small dextrorotatory rotation of (+)31° $dm^{-1}\,g^{-1}\,cm^3$ initially recorded for *trans*-**5R** was further reduced to about (+)9° $dm^{-1}\,g^{-1}\,cm^3$. A specific rotation of (+)26° $dm^{-1}\,g^{-1}\,cm^3$ was recovered after visible light illumination. While these changes were completely reversible over multiple UV light–visible light illumination cycles, the magnitude of this polymer's oscillatory response was clearly attenuated relative to those shown in Fig. 2 for the random copolyesters **7R** and **8R**. Importantly, photostationary state *trans–cis*-isomer compositions residing along each polyester backbone were found to be similar and thus cannot account for the different stimuli-responsive profiles depicted in Fig. 2.

The altered photo-dynamic behavior displayed by copolyester **5R** is entirely consistent with its unique periodic backbone structure. In this construct, the flexible ethylene oxide spacer segments likely serve to insulate the atropisomeric *R*-binaphthylene units along the polymer's main-chain from steric and/or electronic perturbations that are generated by the reversible azobenzene isomerization reactions. It is important to note that comparable insulating or damping effects cannot be operative in the random copolyester variants **7R** and **8R** (or the wholly aromatic analogue **1R**) where neighboring azobenzene and binaphthylene residues are covalently tied together in tight spatial proximity. That no measurable photo-response was observed (Fig. 2) for the low-T_g periodic copolyester **6R** fitted with even longer triethylene oxide spacer elements lends additional support to this notion.

3.5. Oligomeric model compounds

Four oligomeric model compounds endowed with varying degrees of conformational flexibility were also evaluated as part of this study [14]. Derivatives **9R–12R** were synthesized from their corresponding *R*-binaphthylene diols and *trans*-4-(phenylazo)benzoyl chloride in a single step as outlined in Scheme 4. Oligomer *trans*-**9R** lacking ethylene oxide spacer segments was selected to mimic the local backbone structure found in the conformationally restricted polyester *trans*-**1R** while variants *trans*-**10R** through *trans*-**12R** were designed

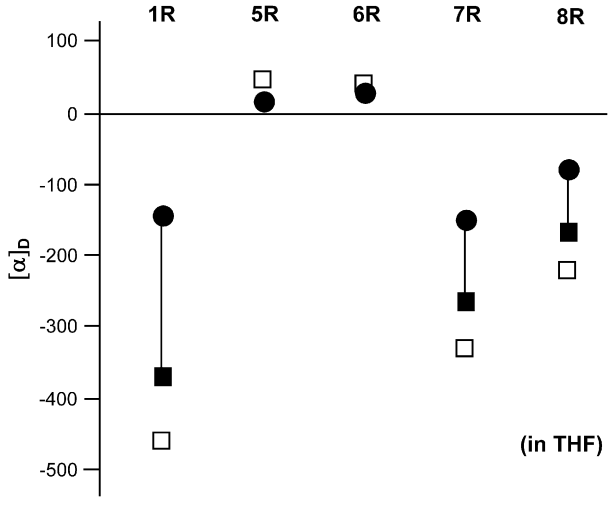

Fig. 2. D-line specific rotations for five polyester analogues dissolved in THF before (□) and after separate UV (●) and visible (■) light exposure steps. The vertical lines indicate the range of the photo-regulated chiroptical response for each system.

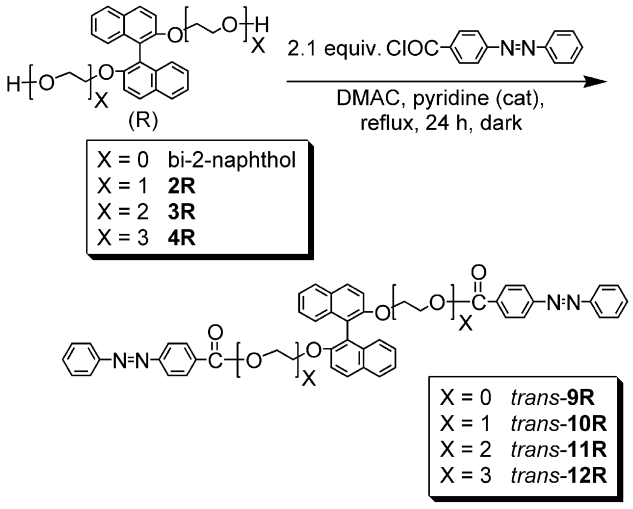

Scheme 4. Synthesis of oligomeric model compounds fitted with (oligo)ethylene oxide spacer elements.

Table 4
D-line specific rotation values for oligomeric model compounds before and after light exposure in THF

Model compound	$[\alpha]_D^{25}$ (deg dm^{-1} g^{-1} cm^3)		
	trans-	+UV[a]	+Vis[a]
9R	(−)193	(−)8	(−)121
10R	(+)39	(−)34	(+)15
11R	(+)39	(+)37	(+)38
12R	(+)20	(+)22	(+)21

[a] UV and visible light exposure times = 15 min.

to more thoroughly model the main-chain sequences found in the periodic copolyester constructs described above.

D-line specific rotations for this homologous series dissolved in THF are provided in Table 4. In their dark-adapted, all-*trans* configurations, **9R**–**12R** exhibited optical rotations that closely paralleled the rotational values belonging to their larger polymeric counterparts listed in the second column of Table 3. For example, *trans*-**9R** was characterized by a strong levorotatory rotation falling near (−)193° dm^{-1} g^{-1} cm^3 which was not unlike that observed for the parent polyester *trans*-**1R**. The rotations recorded for *trans*-oligomers **10R** through **12R** were shifted in each case to small positive values falling under (+)40° dm^{-1} g^{-1} cm^3. These rotations were similar in their respective magnitudes to those displayed by periodic copolyesters *trans*-**5R** and *trans*-**6R**.

The D-line specific rotations measured for the four model compounds in THF following the dual UV light and visible light exposure steps were also remarkably similar to those exhibited by their corresponding copolyester analogues. As can be noted from Table 4, the negative rotation initially observed for oligomer **9R** was diminished by a full order of magnitude following the UV irradiation step that gave rise to a new photostationary state composition enriched in the *cis*-azobenzene isomer. The illumination of **9R** with visible light served to trigger the reverse *cis*-to-*trans* reaction, partially restoring this small compound's optical rotatory power to about (−)121° dm^{-1} g^{-1} cm^3. This reversible photo-modulated response spanned a range of 113° dm^{-1} g^{-1} cm^3 and was qualitatively similar to that tracked earlier for polyester **1R** (see Fig. 1). Vastly diminished photo-induced oscillations in optical rotations were noted for oligomeric model compound **10R** that was fitted with ethylene oxide spacer segments. However, this flexible derivative's initial dextrorotatory rotation actually inverted to the opposite sign following the UV illumination step. A small positive rotation was restored by visible light. It is interesting to note that this chiroptical switching response was not observed for its larger periodic copolyester analogue **5R**. This behavioral difference may stem from longer-range conformational effects along the polymer's main-chain that are not operative in the smaller model compound. Importantly, light directed fluctuations in optical rotations were essentially absent from model compounds **11R** and **12R** where central binaphthylene and terminal azobenzene moieties were separated by longer di- and triethylene oxide segments, respectively. This observation was fully consistent with the absence of photo-modulated output for periodic copolyester **6R** that also possessed "soft" triethylene oxide spacer elements within its polymer backbone.

4. Conclusions

The incorporation of conformationally flexible (oligo)ethylene oxide segments into the main-chain of polyester **1R** resulted in a new family of polymeric materials that possessed a range of photo-responsive chiroptical properties. Light-regulated outputs were found to be strongly dependent upon the length of the flexible backbone segments employed and on their specific locations of placement within the polyester chains. Most notably, the insertion of oligo(ethylene oxide) spacer elements between neighboring *R*-binaphthylene and azobenzene main-chain units had a pronounced damping effect on the photo-dynamic behavior exhibited by these chiral systems. Similar results were noted for a related series of oligomeric model compounds that were specifically designed to represent local monomer sequences present within the larger polyester structures. That the shorter oligomeric model compounds effectively mimicked the chiroptical behavior shown by their larger macromolecular analogues clearly suggests that longer-range conformational geometries provided by higher molecular weight polymeric backbones are not necessarily required for the photo-modulated effects described herein.

The results derived from this study shed additional light on the mechanisms that are responsible for the photo-regulation of optical rotations in materials of this kind. As we reported earlier [3–8], isomerization-induced changes in azobenzene geometry and polarity have the potential to perturb chiral backbone conformations that exist over both local and more global length scales. Reversible alterations in the inter-ring dihedral angle (Φ) characterizing each atropisomeric *R*-binaphthylene backbone segment are of particular importance because these rotational changes are known from numerous studies [18–21] to influence chiroptical behavior. For the polymers and oligomers described above, internal binaphthylene dihedral angles will be sterically and/or electronically sensitive to the nature of the substituents appended to the 2- and 2′-positions of the ring system as depicted in Fig. 3. Thus, the large disparities in the specific rotation values initially recorded for the *trans*-copolyesters with random or periodic backbone sequences can be attributed to different steric or electronic environments flanking the binaphthylene moieties in each of these copolymer constructs. Moreover, the azobenzene stimuliphores present along each copolyester backbone will best function as molecular actuators when they are tightly coupled to neighboring binaphthylene groups. The photo-regulated isomerization process should therefore have its greatest influence on dihedral angles in constructs where azobenzene and binaphthylene groups are covalently tied together. As flexible spacer elements of increasing length are inserted into these systems, the influence of the azobenzene stimuliphores will become progressively diminished and

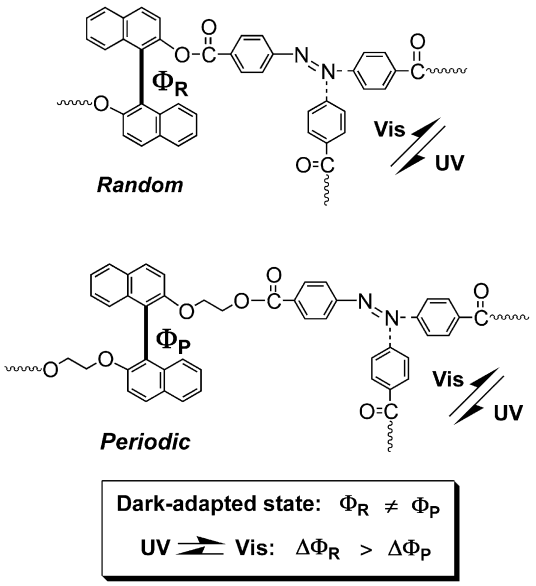

Fig. 3. Proposed scheme depicting how the *R*-binaphthylene segment's dihedral angle (Φ) might be influenced by either a random or a periodic sequence of monomer units along the polyester chain both before and after the light exposure steps.

photo-induced oscillations in optical rotatory power should gradually be screened or dampened out.

The structure–property relationships gathered from this study are also useful in that they provide guidance for the rational design of newer stimuli-responsive materials with different behavioral attributes. For example, the use of additional comonomer sequences to influence polymer solubilities, T_g values or other material properties can be well tolerated as long as their presence along the polymer chain does not disrupt the covalent connectivity of adjacent binaphthylene and azobenzene backbone units. Targeted efforts to prepare a new series of block copolyesters fitted with low-T_g poly ethylene oxide segments that might be capable of exhibiting light-modulated chiroptical properties in rubbery, solid-state environments are currently underway and the results from these efforts will be described in a future communication.

Acknowledgments

The author wishes to thank Eric D. Felton, Robert A. Pryor, Mimi Y. Keating (DuPont) and Gerry J. Everlof (Bristol-Myers Squibb Co.) for their help with some of the analytical procedures described herein. The constructive comments offered by several reviewers of this paper are also warmly acknowledged. This study is part of a larger program on stimuli-responsive polymers and materials systems and is DuPont Contribution No. 8748.

References

[1] Pu L. Chem Rev 1998;98:2405.
[2] Howe LA, Jaycox GD. J Polym Sci Part A Polym Chem 1998;36:2827.
[3] Everlof GJ, Jaycox GD. Polymer 2000;41:6527.
[4] Lustig SR, Everlof GJ, Jaycox GD. Macromolecules 2001;34:2364.
[5] Jaycox GD. Structured polymers with stimuli-responsive behavior – azobenzene modified helical constructs. In: Khan IM, editor. Synthetic macromolecules with higher structural order. ACS symposium series 812. Washington DC: American Chemical Society; 2002 [chapter 7].
[6] Jaycox GD. Polym J 2002;34:280.
[7] Jaycox GD. J Polym Sci Part A Polym Chem 2004;42:566.
[8] Jaycox GD. J Polym Sci Part A Polym Chem 2006;44:207.
[9] Kondo F, Takahashi D, Kimura H, Takeishi M. Polym J 1998;30:161.
[10] Kondo F, Kakimi S, Kimura H, Takeishi M. Polym Int 1998;46:339.
[11] Pieraccini S, Masiero S, Spada GP, Gottarelli G. Chem Commun 2003; 598.
[12] Unpublished results, this laboratory; 2006.
[13] Jaycox GD. Polym Prepr (Div Polym Chem, ACS) 2005;46(2):963.
[14] Jaycox GD. Polym Prepr (Div Polym Chem, ACS) 2005;46(2):965.
[15] Jaycox GD. Polymer 1998;39:2589.
[16] Stock HT, Kellogg RM. J Org Chem 1996;61:3093.
[17] Kyba EP, Gokel GW, de Jong F, Koga K, Sousa LR, Siegel MG, et al. J Org Chem 1977;42:4173.
[18] Mislow K, Glass MAW, O'Brien RE, Rutkin P, Steinberg DH, Weiss J, et al. J Am Chem Soc 1962;84:1455.
[19] Mason SF, Seal RH, Roberts DR. Tetrahedron 1974;30:1671.
[20] Rosini C, Rosati I, Spada GP. Chirality 1995;7:353.
[21] Di Bari L, Pescitelli G, Salvadori P. J Am Chem Soc 1999;121:7998.
[22] Kumar GS, Neckers DC. Chem Rev 1989;89:1915.
[23] Kumar GS. Azo functional polymers. Lancaster, PA: Technomic; 1992.